INTERNATIONAL ATOMIC ENERGY AGENCY
UNITED NATIONS EDUCATIONAL, SCIENTIFIC AND CULTURAL ORGANIZATION

INTERNATIONAL CENTRE FOR THEORETICAL PHYSICS
34100 TRIESTE (ITALY) - P.O.B. 586 - MIRAMARE - STRADA COSTIERA 11 - TELEPHONE: 2240-1
CABLE: CENTRATOM - TELEX 460392-1

H4.SMR/204 - 29

WINTER COLLEGE ON

ATOMIC AND MOLECULAR PHYSICS

(9 March - 3 April 1987)

ATMOSPHERIC DIAGNOSTICS I

U. Platt

Kernforschungsanlage Jülich GMBH
Jülich
West Germany

Lectures at the ICTP winter college on
"DIAGNOSTIC ATOMIC AND MOLECULAR SPECTROSCOPY"

Ulrich Platt, Kernforschungsanlage Jülich, ICH 3
D-5170 Jülich, W. Germany

Abstracts of the lectures on 'Atmospheric Diagnostics I'

1st LECTURE - INTRODUCTION TO THE ATMOSPHERE:

Physical properties of the atmosphere:
Layering of the atmosphere, thermal structure, turbulent structure
(troposphere/stratosphere/thermosphere etc.).
Dynamics of the atmosphere, global and regional transport.

Chemical properties of the atmosphere:
Composition of the atmosphere, lifetime of trace gases.
Radiation and photochemistry.
Stratospheric ozone (Chapman cycle, ozone destruction mechanisms)
Tropospheric trace gas cycles, primary and secondary trace gases.
(role of free radicals, photochemistry)
Tropospheric Ozone
Thermodynamics of atmospheric reactions.
Atmospheric Aerosols

2nd LECTURE - ATMOSPHERIC MONITORING

Interaction of electromagnetic radiation with atoms and molecules.
Vibrational and rotational structures of molecular absorption.
Principles of spectroscopic trace gas measurement techniques.
Lambert Beer's law.

Categories by physical principle
- Absorption spectroscopy (UV/Visible, IR, microwave)
- Emission spectroscopy (thermal emission of IR-, microwave-radiation)
- Fluorescence/Chemiluminescence (laser induced fluorescence, airglow)

Categories by technical arrangement
- Active methods (LIDAR, DOAS, LIF)
- Passive techniques (emission spectroscopy, solar backscatter, solar occultation)

Spectroscopic instruments

3rd LECTURE - SPECTROSCOPIC TECHNIQUES I

Active ground based applications of spectroscopic techniques (except LIDAR)
Description of techniques, instruments, applications, and results.

- Differential optical absorption spectroscopy (DOAS)
- Long path FT-IR spectroscopy.
- Tunable diode laser spectroscopy (TDLS)
- Laser induced fluorescence (LIF)

Sample results

4th LECTURE - SPECTROSCOPIC TECHNIQUES II

Ground based passive remote sensing:

Total column measurements
direct solar visible/UV (occultation experiments, DOBSON spectrometer etc.)
Twilight observations.
Airglow (atmospheric oxygen bands)

Satellite measurements:

Solar UV backscatter
Limb scanning
Occultation
Measured 'phenomena' (trace gas concentration, temperature, pressure wind speed)

Sample results

Atmospheric Chemistry –

Atmospheric Diagnostics

- Scientific Reasons

- Assessment of anthropogenic changes in atmospheric composition - consequences.
  - Climatic change
  - Ozone layer (South pole !)
  - Perturbations in global tropospheric chemistry (increase of O_3(!), CH_4, CO, N_2O)
  - Habitability of urban areas

Thermal Structure of the Atmosphere

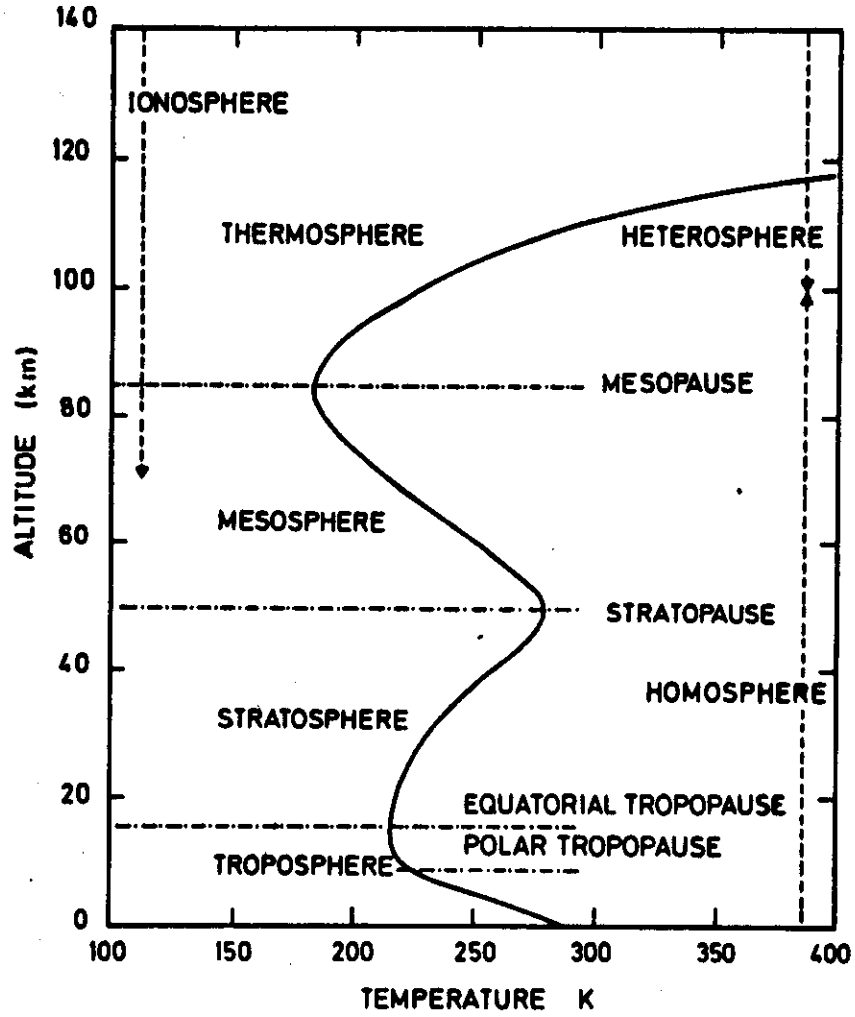

Fig. 3.1. Thermal structure of atmospheric layers.

Chapman Ozone" versus Reality

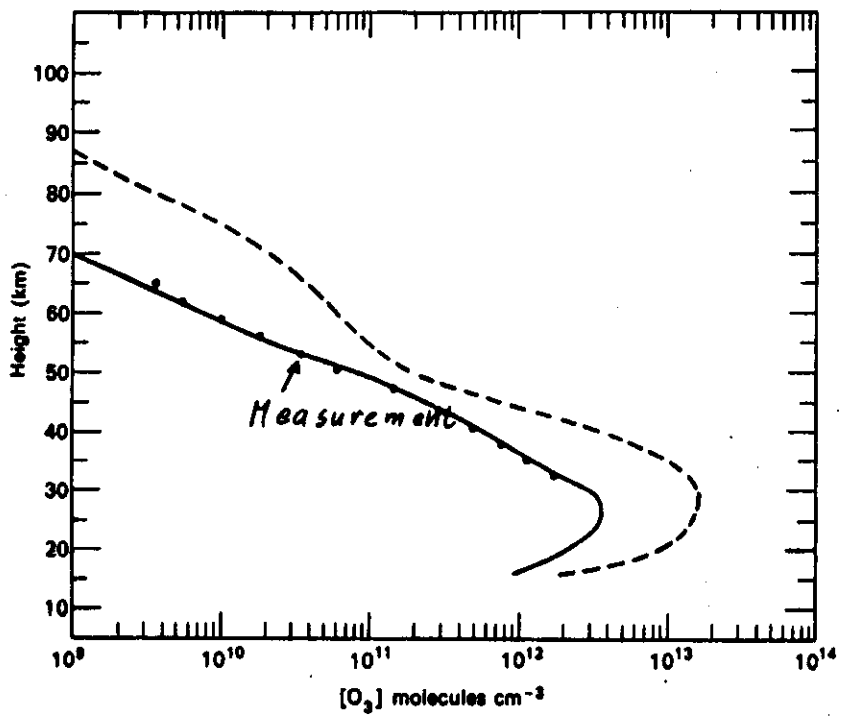

Fig. 4.3 A comparison of a photochemical profile of O_3 for an oxygen only atmosphere[12] (dashed line) with the experimental results of Johnson *et al.*[13] (solid curve) and Hilsenrath (dotted curve).[13]

The Chapman Cycle:

$$O_2 + h\nu \longrightarrow O + O$$
$$O + O_2 + M \longrightarrow O_3 + M \quad \Big\} \; O_3 \text{ - Formation}$$

$$O_3 + h\nu \longrightarrow O + O_2$$
$$O + O_3 \longrightarrow O_2 + O_2 \quad \Big\} \; O_3 \text{ - Destruction}$$

Catalytic O_3 - Losses:

$$O_3 + X \longrightarrow XO + O_2$$
$$O + XO \longrightarrow X + O_2 \quad \Big\} \; X = OH, NO, Cl \; (XO = HO_2, NO_2, ClO)$$

$$\text{Net:} \quad O + O_3 \xrightarrow{X} O_2 + O_2$$

Rotational - Vibrational Structure of Electronic - Molecular Spectra

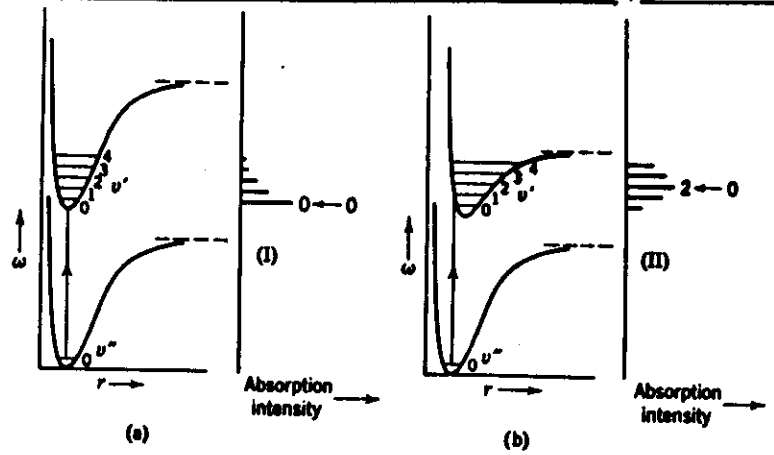

Fig 3-25 Typical potential energy curves for different types, I and II, of band spectra.

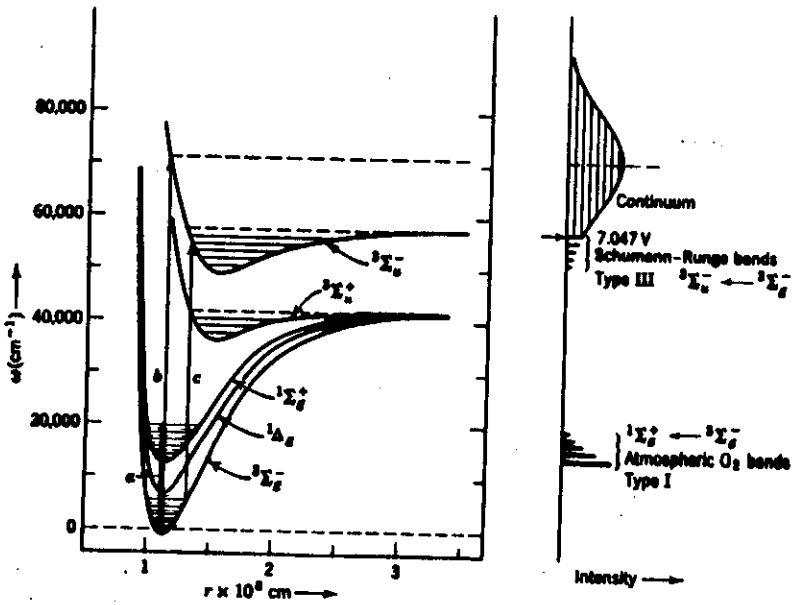

Fig. 3-27 Franck-Condon curves for the O_2 molecule; the paths for the formation of the atmospheric O_2 absorption bands, the Schumann-Runge bands, and the O_2 continuum are shown. Relative absorption band intensities within each transition are shown, but the intensities of the two electronic transitions are not to scale, the $^3\Sigma_u^- \leftarrow {}^3\Sigma_g^-$ being far more intense than the $^1\Sigma_g^+ \leftarrow {}^3\Sigma_g^-$. From Herzberg,[1] pp. 194, 195.

Common Principle of all Techniques

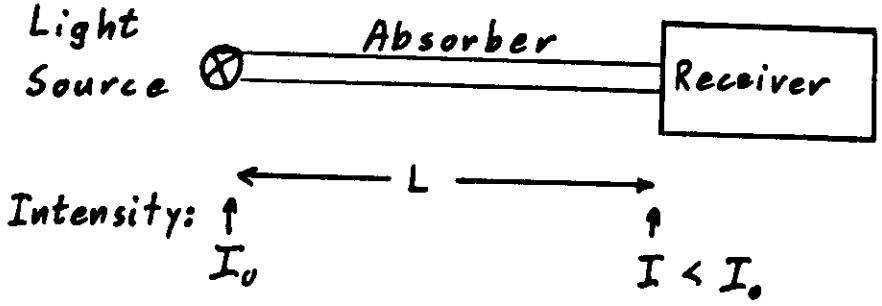

Light extinction:

$$I = I_0 \cdot e^{-c \cdot L \cdot \varepsilon}$$

Trace gas concentration c:

$$c = \frac{1}{L \cdot \varepsilon} \cdot \underbrace{\mathrm{Log}\left(I_0 / I\right)}_{\text{optical density}}$$

ε = constant, characteristic for species and wavelength

Example: Bromine-oxide free radical (Type II)

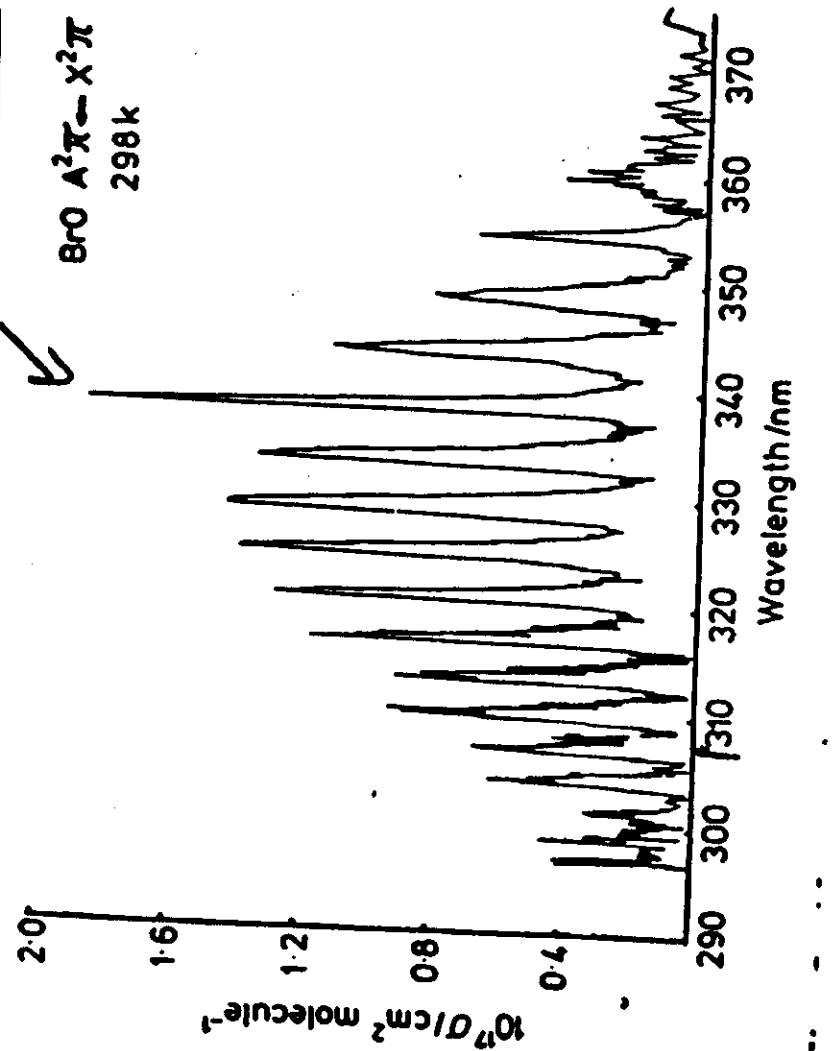

Measurement of Atmospheric Trace Gases by Optical Absorption Spectroscopy

Techniques in use can be categorised by:

- Wavelength (UV - visible - IR)
- Light path arrangement:
  - 'long path'
  - folded path (once, many times)
  - reflector type: mirror
    - 'topological target'
    - aerosol - molecules (Lidar)
- Light Source:
  - thermal (incandescent lamp, arc lamp, sun, moon, stars)
  - LASER (narrow / wide - band)
    - Dye -, Diode -, CO_2 - LASER
- Light receiving system:
  - dispersive (rapid scan, diode array, derivative, mask correlation)
  - Fourier transform
  - Hadarmad transform

(DOAS - low res.)

(...

Satellite Measurement of Atmospheric Trace Gases

Advantage: Rapid coverage of a large area

Problem Large distance from the investigated object

Techniques:

Solar Occultation: Use direct sunlight during "sunrises / sunsets" seen by the satellite.

Solar Backscatter: Use scattered sunlight (UV/visible)

Examples:
- SME: NO_2 at $\lambda = 430 - 450$ nm
- DE-1: O_3 at $\lambda = 317.5 / 360$ nm
- NIMBUS-4: O_3 at $\lambda = 312 - 380$ nm
- NIMBUS-7: SO_2 at $\lambda = 290 - 310$ nm

Thermal IR-Emission: Use (IR)-light emitted by atmospheric constituents

Example: NIMBUS-7-LIMS:
O_3, HNO_3, H_2O, NO_2, Temperature from IR, $\lambda = 6{,}2 \ldots 15\,\mu m$

From:

Optical and Laser Remote Sensing

D.K. Killinger + A. Mooradian Eds.

Springer Verlag Berlin, Heidelberg, New York 1983

2.6 Measurements of Atmospheric Trace Gases by Long Path Differential UV/Visible Absorption Spectroscopy

U. Platt* and D. Perner

Kernforschungsanlage Jülich, Institut für Chemie 3, Atmosphärische Chemie, D-5170 Jülich, Fed. Rep. of Germany

Introduction

Absorption spectroscopic measurement methods for trace gas analysis have a number of clear advantages over sampling methods, including absence of wall losses, greater specificity and the potential for real time measurements of several different species with a single type of instrument. Nonetheless, only a relatively small number of spectroscopic measurements of atmospheric trace gases have been reported in the past, using infrared or UV/visible absorption spectroscopy (Hanst 1971, Tuazon et al. 1981, Connell et al. 1980, Noxon et al. 1980, 1981, Bonafé et al. 1976, Millán et al. 1978).

The present paper describes a relatively simple instrument capable of detecting and measuring a number of important trace gases at tropospheric concentration levels by observing their structured UV/visible absorption features. The absorption is monitored over a long, open air path stretching several kilometers between an artificial light source and the receiving system containing the spectrometer. This setup ensures the coverage of a large air volume by the instrument.

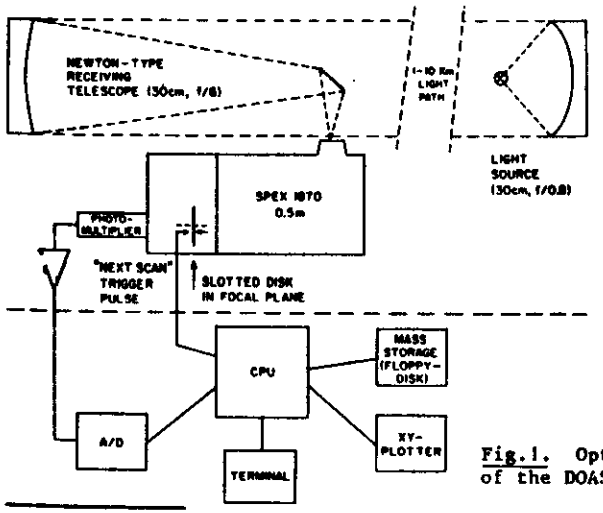

Fig.1. Optical and electronic setup of the DOAS system

*Present Address: Statewide Air Pollution Research Center
University of California, Riverside, CA 92521

The Differential Optical Absorption (DOAS) Spectrometer

Optical Setup. The basic DOAS system optical setup monitors the absorption of atmospheric trace gases contained in a long (~1-10 km) optical path, it therefore consists of two separate units (Figure 1):

(1) The light source, designed to emit a parallel beam of light, free of spectral structure in the wavelength ranges of interest (i.e., emitting "white" light). This is accomplished by either using Xe-high pressure lamps (Osram XBO 450, Hanovia 959C1980) or incandescent lamps (150-240 W quartz iodine) in combination with a "search light" type focussing mirror (0.3 m diameter, 0.25 m focal length) or, in special cases a frequency doubled CW-dye-laser.

(2) In the receiving unit at the other end of optical path, the light is collected by a Newton-type telescope and focussed into the entrance slit of a spectrograph. Instruments with focal lengths from 0.2 to 0.85 m equipped with 600-2160 groove/mm gratings are being used, depending on the required resolution. Also a minicomputer with appropriate peripherals (PDP 11/2 or 11/23) is an integral part of the instrument.

The Rapid Scanning Device. A 6 to 40 nm segment of the dispersed spectrum produced in the exit focal plane of the spectrograph is scanned by a series of moving exit slits etched radially in a thin metal disk (slotted disk) rotating in the focal plane. At a given time, one particular slit is used as an exit slit. The light passing through the exit slit is received by a photomultiplier tube, the output signal of which is digitized by a high-speed analog-to-digital converter and read by a minicomputer. During one scan (i.e., one sweep of an exit slit over the spectral interval of interest), several hundred digitized signal samples are taken. Consecutive scans are performed at a rate of approximately 100 scans per second and are signal averaged by the software.

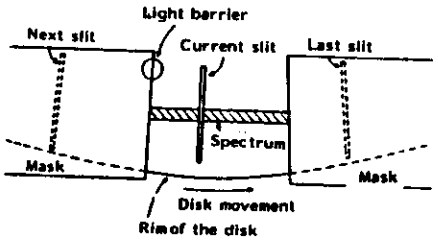

Fig.2. The "slotted disk" rapid scanning device located in the focal plane of the spectrometer

The process of taking one spectral scan and the interaction of hardware and software thereby is best illustrated in conjunction with Figure 2. The central wavelength of the scan is selected by the spectrograph setting and the width of the scan region by a mask located very close to the slotted disk. The distance between the slits along the rim of the disk is slightly larger than the aperture of the mask, so that at any time no more than one slit is irradiated. As a slit becomes visible at the left edge of the mask, it is detected by an infrared light barrier located there (see Figure 2), and a trigger signal is sent to the computer. While the slit then sweeps over the spectrum, the computer continuously takes digitized samples of the light intensity at the current position of the slit. Thus, one sweep of a slit is divided into several hundred channels, each associated with a wavelength interval several times narrower than the resolution of the spectrograph. During each scan, the digitized samples are added to the corresponding channels in the computer memory, thereby all consecutive scans are superimposed in the computer memory (signal averaged).

After finishing one scan, the computer waits for the next trigger pulse to indicate the next slit (shown in dashed lines in Figure 2) approaching the left edge of the mask. In order to preserve the spectral resolution while superimposing a large number of individual scans, the rotational speed of the slotted disk is kept constant to within ± 0.1%. The signal variations seen by the computer during a single spectral scan can be caused by several effects:

(1) The light absorption by trace gases varies with wavelength.
(2) The light losses due to mirror reflectivities, etc., may vary with wavelength.
(3) The output of the light source may vary with wavelength and time.
(4) Atmospheric refraction may change with time (due to turbulence).
(5) Random noise is added to the signal by the photomultiplier, preamplifier and A/D converter.

Since a single scan takes less than 10 msec, the effect of atmospheric scintillations is very small, because the frequency spectrum of atmospheric turbulence close to the ground peaks around 0.1-1 Hz and contains very little energy at frequencies above 10 Hz (Haugen 1973). In addition, typical spectra obtained during several minutes of integration time represent an average over 10-40 thousand individual scans. Thus, effects of noise and temporal signal variations are very effectively suppressed. In fact, even momentarily blocking the light beam entirely (e.g., due to a vehicle driving through the beam) has no noticeable effect on the spectrum.

Due to the very narrow field of view of the instrument (approximately $0.3\ 10^{-4}$ by $1.1\ 10^{-4}$ steradians), solar stray light levels have been found to be extremely low, with the exception of very hazy conditions. In the latter cases, however, the stray light can easily be cancelled by frequently interrupting the measurement and taking a "straylight spectrum" with the telescope pointed beside the light source. Since only an offset of a fraction of a degree is required, this does not change the amount of stray light entering the system, which then can then be subtracted from the total spectrum.

Remaining undesired influences on the shape of the spectrum are eliminated by the mathematical treatment of the spectrum and the way the information on trace gas concentration is extracted, as discussed below.

Processing of Absorption Spectra

Usually the raw spectra will show an overall slant caused by slight variations of lamp output or atmospheric scattering over the observed wavelength interval. In order to remove this overall feature, a polynomial (first to fifth order) is fitted to the spectrum and subsequently the spectrum is divided by this polynomial. The "narrow" features (extending only over a narrow wavelength range) caused by trace gas absorption are not much affected by the process.

The trace gas concentration C is, as usual with optical methods, derived from the spectrum by applying Beer's law:

$$C = (\log I_0/I)/(\varepsilon L) \qquad (1)$$

where I_0 = light intensity without absorption by the trace gas
I = light intensity, reduced due to absorption by the trace gas
ε = absorption coefficient of the trace gas
L = length of the light path .

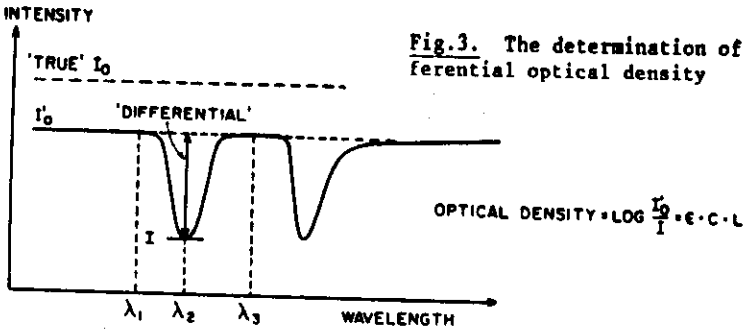

Fig.3. The determination of the differential optical density

Since the true light intensity I_0, without any absorption, cannot be obtained with this method (see Figure 3), the "differential" optical density is used to evaluate the trace gas concentration. The differential optical density is defined by log I'_0/I where I'_0 is the intensity (at wavelength λ_2) in the absence of the particular absorption structure, rather than in the absence of any absorption at all (as indicated by the dashed line in Figure 3). According to this definition, I'_0 can be calculated from $I(\lambda_1)$ and $I(\lambda_3)$:

$$I'_0 = I(\lambda_1) + [I(\lambda_3)-I(\lambda_1)] \cdot \frac{\lambda_2-\lambda_1}{\lambda_3-\lambda_1} \qquad (2)$$

Of course, the absorption coefficient ε has to reflect the above definition of I'_0, accordingly the "differential absorption coefficient" of a trace gas will generally be lower than the total absorption coefficient at the same wavelength.

In the practical application of the instrument, the precision of the measurements is improved by least squares fitting a reference spectrum of the substance under consideration to the observed absorption spectrum, thus all absorption bands of a given substance in the scanned spectral region, as well as the information contained in their relative strengths and particular shapes (the "fingerprint" of the substance), are used. This method even allows the deconvolution of overlapping spectra of different species to obtain the concentration of the contributing components with good accuracy. Examples of this process will be given below.

Software

The software for the DOAS spectrometer performs three major tasks (Figure 4):

(1) The individual spectral scans are signal averaged in the computer memory and displayed on an oscilloscope screen.

(2) System housekeeping (e.g., monitoring signal intensity, counting of scans, etc.) is carried out as a "background" task.

(3) A large number of mathematical functions can be applied to the acquired absorption spectra in order to extract the trace gas concentrations from the spectra. Also, spectra can be stored and recalled on mass storage devices (e.g., disks).

The program is written in MACRO 11 and FORTRAN IV for use with Digital Equipment PDP 11 computers.

The mathematical functions available for manipulation of the absorption spectra include multiplication and division by a constant factor,

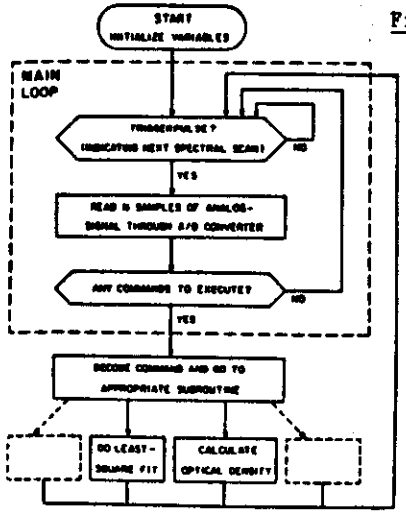

Fig.4. DOAS program flow chart

addition and subtraction of two spectra, division by a least square fitted polynomial, shifting the spectra in wavelength, change of the wavelength scale ("expansion" and "compression" of a spectrum), calculation of the differential optical density of an indicated absorption band, least square fitting of up to four reference spectra to a given spectrum, and taking the logarithm of a spectrum.

In addition to that, several hardware functions like changing the wavelength setting of the spectrometer or moving a filter into the light path are controlled by the software. All software functions can be executed in automatic sequences, thus allowing unattended operation of the instrument.

Detection Limits of the DOAS System

The detection limit for a particular substance can be calculated according to equation (1), if the differential absorption coefficient, the minimum detectable optical density (OD) and the length of the light path are known. While for a given minimum detectable OD the detection limit improves proportionally to the length of the light path, this does not mean that the actual detection limit always improves with a longer light path. This is because with a longer light path the received light intensity $I(\lambda)$ tends to be lower, increasing the noise associated with the measurements of $I(\lambda)$ and thus increasing the minimum detectable OD. A few simple considerations may clarify this relationship and also allow the derivation of detection limits.

The amount of light emitted by a search-light type light source (see Figure 1) varies enormously with power and type of lamp, as well as with focal length and size of the mirror. However, the size of the light emitting area of the lamp and the focal length of the mirror only affect the divergence of the beam. Thus the intensity of the beam (in W/sr) only depends on the luminous intensity of the lamp (W/mm^2) and the area of the mirror.

Furthermore, the size of the light source image projected onto the entrance slit of the spectrometer by the receiving system is proportional

to the size of the light source mirror, the focal length of the telescope, and inversely proportional to the distance L between light source and receiving system. Nothing is gained by making the light source image larger than the height of the entrance slit, thus for given light path and slit dimensions, the maximum usable light source mirror size and receiving telescope focal length are also determined (and thereby the mirror diameter, since it has to match the aperture of the spectrometer).

For a typical DOAS system with an 0.3 m diameter, 1.8 m focal length receiving telescope and 0.2 mm entrance slit height, there are no geometrical light losses up to path lengths of about 3 km (for longer light paths, the size of the light source mirror could easily be increased, since an inexpensive metal mirror can be used here). However, in addition to geometrical light losses, light attenuations due to atmospheric absorption as well as to scattering affect the magnitude of the received light signal:

$$I_{received} = I_{source} \cdot \exp(-L/L_0) \qquad (3)$$

where the absorption length L_0 reflects the combined effects of broad band atmospheric absorption and Mie- and Rayleigh scattering.

Since the noise level of a photomultiplier signal is essentially dependent on the number of photons received and thus is proportional to the square root of the light intensity. The signal-to-noise ratio of a DOAS system as a function of the light path length L can be expressed as:

$$S/N \sim L \exp(-L/2L_0) \qquad (4)$$

This relationship holds for the case of "no geometrical light losses" and yields an optimum S/N ratio for a light path length $L = 2\,L_0$. While there are no lower limits for L_0 in the atmosphere (fog), the upper limits are given by Rayleigth scattering, and the scattering by atmospheric background aerosol which indicate optimum light path lengths ($2\,L_0$) in excess of 10 km for wavelengths above 300 nm.

With a typical DOAS system (using an Xe light source), for wavelengths > 300 nm minimum detectable optical densities of (5-10) 10^{-5} (base 10) can be achieved in a few minutes of averaging time. The minimum detectable OD can be higher, if it is necessary to subtract overlapping absorption features of other species (see below); however, in most practical cases, the detection limits are only slightly degraded, since overlapping bands can usually be removed to 99-99.9%. Thus, to noticeably increase the detection limit, the overlapping absorption must be ~100 times stronger than the absorption under consideration. Table 1 gives detection limits for a number of atmospheric trace constituents, for a 10 km ground based light path and a minimum detectable OD of 10^{-4}. The detection limits are usually in the part per trillion (ppt) range, and for studies in polluted air much shorter light paths (e.g., 1-3.5 km) have been used. All substances in Table 1 have already been observed in the ambient atmosphere (Platt et al. 1979, Perner and Platt 1979, Platt et al. 1980a,b,c, Platt et al. 1981, Harris et al. 1982).

Absorption Spectra of Substances Important to Tropospheric Chemistry

Figures 5 through 7 show examples of absorption spectra of trace gases which are important in the polluted as well as in the unpolluted troposphere. Nitrous acid (HONO) and the nitrate radical (NO_3) have been detected in the troposphere for the first time using this method.

Table 1. Atmospheric Trace Components Observed by Differential UV-VIS Spectroscopy

Substance	Wavelength Range [nm]	Differential Absorption Coefficient[a] [cm^2/molec]	[at nm]	Detection for 10 km Light Path [ppt]
SO_2	200-230,290-310	5.7×10^{-19}	300	17
CS_2	200-220,320-340	4×10^{-20}		240
NO	215,226	2.3×10^{-18}	226	400[b]
NO_2	330-500	1.0×10^{-19}	363	100
NO_3	623,662	1.8×10^{-17}	662	0.5
HNO_2	330-380	4.2×10^{-19}	354	20
O_3	220-330	4.5×10^{-21}	328	2100
HCHO	250-360	7.8×10^{-20}	340	120
OH	308	2×10^{-16}[c]	308	0.05

[a] 0.3 nm, spectral resolution; [b] 1 km light path, minimum detectable O.D. = 10^{-3}; [c] 0.003 nm spectral resolution

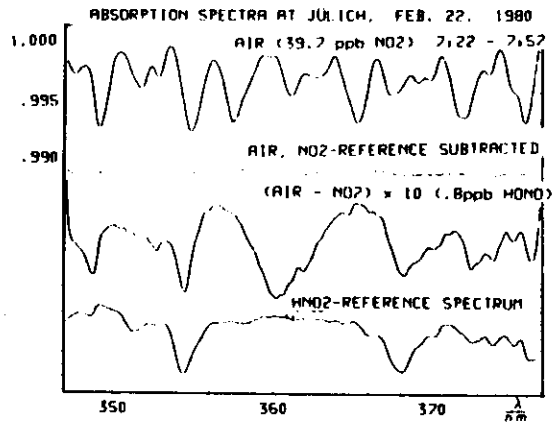

Fig.5. Deconvolution process of an air spectrum (taken at Jülich, Germany, 3.5 km light path) showing NO_2 and HONO absorption features

Figure 5 shows the spectral region from 348 through 378 nm in which NO_2 and HONO are the dominant absorbing species. The uppermost trace in Figure 5 shows the "air" spectrum which is almost entirely due to NO_2. After the subtraction of a suitably weighted NO_2 reference spectrum, the residual spectrum is an almost featureless trace. The next trace (third from top, Figure 5) is identical to the second, with 10 times expanded vertical scale. Here the absorption bands of nitrous acid (354 nm and 368 nm) become clearly visible, agreeing well in position and shape with the pure HONO reference shown in the lowest trace. In addition, the strong, wide absorption feature at 360 nm is due to the light absorption by collision pairs of oxygen $(O_2)_2$ (Perner and Platt 1980).

The example in Figure 6 covers the wavelength region from 325 nm to 350 nm, where the most dominant absorption usually is due to NO_2, and additional absorption features of ozone and formaldehyde are observed.

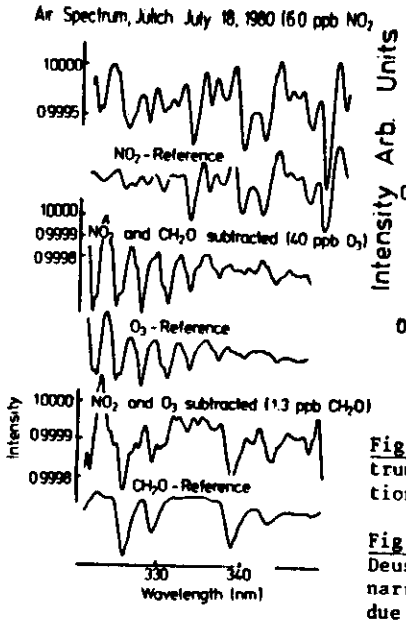

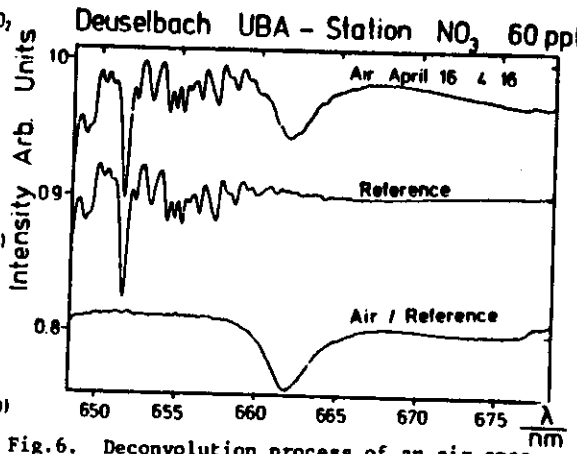

Fig.6. Deconvolution process of an air spectrum with overlapping NO_2, O_3 and HCHO absorptiors

Fig.7. NO_3 spectrum (60 ppt NO_3) taken at Deuselbach, Germany, 4.8 km light path. The narrow features between 650 and 660 nm are due to water vapor

The spectrum in Figure 6 was taken under moderately polluted conditions in Jülich, Germany and shows (from top to bottom) three pairs of traces: (1) air spectrum and NO_2 reference spectrum, (2) air spectrum with fitted amounts of NO_2 and HCHO subtracted, leaving the ozone absorption feature, and a pure ozone reference spectrum, (3) air spectrum with fitted amounts of NO_2 and ozone subtracted, leaving the formaldehyde absorption features as compared with a pure formaldehyde reference spectrum.

In practice, of course, the concentrations of all three contributing species (NO_2, O_3, HCHO) are obtained in one step by simultaneously fitting the reference spectra to the air spectrum. The procedure shown in Figure 6 of partial subtraction of features, however, provides a good test of whether the fit works properly and also shows, in this case, that no other absorptions are present in the spectrum.

The last example (Figure 7) shows one absorption line of the nitrate radical (NO_3) at 662 nm. Here the feature is already clearly visible in the air spectrum (taken at Deuselbach, Germany). However, some overlap occurs with strong water bands in the 650 to 660 nm range. Since the nitrate radical concentration is extremely low at daytime due to its rapid photolysis (Magnotta and Johnston 1981), a daytime spectrum can be taken as a reference to ratio out the water lines, as shown in the lowest trace of Figure 7.

The application of the DOAS system to studies of trace pollutants and atmospheric constituents in the Los Angeles Basin is described in a companion paper (Harris et al. 1982).

Conclusion

In several years of practical use for the measurement of ambient trace gas concentrations, DOAS systems have been proven to be reliable and adaptable instruments. Continuing efforts to improve the system are aimed using a folded path (White optical system) and the expansion of the number of detectable trace constituents. Atmospheric components likely to be detectable by DOAS instruments, in addition to those already observed, include benzaldehyde, C_2H_2, NH_3 and the ClO radical.

References

Bonafé, G. Cesari, G. Giovanelli, T. Tirabassi and O. Vittori, Atmos. Environ., 10, 469-474 (1976).

Connell, P. S., R. A. Perry and C. J. Howard, Geophys. Res. Lett., 7, 1093-1096 (1980).

Hanst, P. L., Adv. Environ. Sci. Technol., 2, 91 (1971).

Harris, G. W., W. P. L. Carter, A. M. Winer, J. N. Pitts, Jr., U. Platt and D. Perner, Env. Sci. Technol., in press (1982).

Harris, G. W., A. M. Winer and J. N. Pitts, Jr., Presented at Workshop on Optical and Laser Remote Sensing, Monterey, CA, February 9-11, 1982 (following paper).

Haugen, D. A. (editor), Workshop on micrometeorology, Science Press, Ephrata, PA (1973).

Millán, M. M. and R. M. Hoff, Atmos. Environ., 12, 853-864 (1978).

Noxon, J. F., R. B. Norton and W. R. Henderson, Geophys. Res. Lett., 7, 125-128 (1980).

Noxon, J. F., Geophys. Res. Lett., 8, 1223-1226 (1981).

Perner, D. and U. Platt, Geophys. Res. Lett., 6, 917-920 (1979).

Perner, D. and U. Platt, Geophys. Res. Lett., 7, 1053-1056 (1980)

Platt, U., D. Perner and H. W. Paetz, J. Geophys. Res., 84, 6329-6335 (1979).

Platt, U., D. Perner, A. M. Winer, G. W. Harris and J. N. Pitts, Jr., Geophys. Res. Lett., 7, 89-92 (1980a).

Platt, U., D. Perner, A. M. Winer, G. W. Harris and J. N. Pitts, Jr., Nature, 285, 312-314 (1980b).

Platt, U. and D. Perner, J. Geophys. Res., 85, 7453- (1980c).

Platt, U., D. Perner, J. Schroeder, C. Kessler and A. Toennissen, J. Geophys. Res., 86, 11965-11970 (1981).

Tuazon, E. C., A. M. Winer and J. N. Pitts, Jr., Environ. Sci. Technol., 15, 1232-1237 (1981).

2.7 Measurements of HONO, NO_3, and NO_2 by Long-Path Differential Optical Absorption Spectroscopy in the Los Angeles Basin

G.W. Harris, A.M. Winer, and J.N. Pitts, Jr.

Statewide Air Pollution Research Center and Department of Chemistry, University of California, Riverside, CA 92521, USA

U. Platt and D. Perner

Kernforschungsanlage Jülich, Institut für Chemie 3, Atmosphärische Chemie, D-5170 Jülich, Fed. Rep. of Germany

Introduction

In recent years, atmospheric chemists and air pollution researchers have increasingly looked beyond the "criteria" pollutants (i.e., those for which air quality standards have been established) such as ozone (O_3), nitrogen dioxide (NO_2), sulfur dioxide (SO_2) and carbon monoxide (CO). Thus, interest has grown in the unambiguous identification and measurement of such species as nitric (HNO_3) and nitrous (HONO) acids, formaldehyde (HCHO), the nitrate radical (NO_3), the hydroxyl radical, etc. Of particular concern have been the trace nitrogenous species and the need to assess their roles in the chemical cycles of the clean and polluted troposphere, as well as their impacts on biological systems, including human health and vegetation. Recently, the emerging issue of nitrogenous "acid rain" has accelerated interest in these compounds.

Detailed in situ study of many of the trace compounds in the atmosphere has awaited the development of instruments with the requisite specificity and sensitivity. The measurement of stable compounds and radical intermediates, which may be present at part per trillion (ppt) to part per billion (ppb) concentrations in the complex atmospheric system, presents a challenging analytical problem. Beginning in the mid-1970s, researchers at the Statewide Air Pollution Research Center (SAPRC) undertook a program designed to establish the temporal and geographical distribution of trace pollutants in the Los Angeles air basin. This investigation was originally based on the application of kilometer pathlength Fourier transform infrared (FT-IR) spectroscopy using a Michelson interferometer interfaced to an eight-mirror multiple reflection cell with a base path of 22.5 m (1,2). That system yielded the first spectroscopic detection of HNO_3 and HCHO in the polluted troposphere, as well as detailed simultaneous measurements of ambient concentrations of formic acid (HCOOH), peroxyacetyl nitrate (PAN), ammonia and O_3 (1-4).

Since 1979, we have utilized a second long path technique to complement our FT-IR studies. This technique, differential optical (UV/visible) absorption spectrometry (DOAS), was initially developed by researchers at the Institut für Chemie, Jülich, West Germany (5,6). A detailed description of the DOAS system is given in a companion paper (7). Here we describe the application of this spectrometer to the detection and measurement of trace nitrogenous pollutants in the Los Angeles airshed. Emphasis will be given to our measurements of HONO and NO_3, two species which have been included in models of the chemistry of the atmosphere for many years but which we have only recently characterized for the first time in the polluted troposphere using the DOAS technique (8-10).

DOAS Field-Study Methodologies

In any program of atmospheric monitoring, the technology employed must be practical in a field environment. Thus, for example, wet chemical methods for analyzing air pollutants may be reliable in the laboratory but generally suffer from a number of drawbacks when applied to atmospheric measurements. If a specific procedure is required for each of several atmospheric species, it is unlikely that rapid, simultaneous, multi-component data acquisition will be possible. Moreover, the time required for analyses may be long compared to the characteristic times for changes in the concentration of the species under study and hence only "averaged" rather than "dynamic" information will be available. Finally, the problem of interferences due to gas phase or particulate co-pollutants may be serious for both instrumental and wet chemical analyses.

Broad band (or tuneable narrow band) optical absorption techniques such as DOAS (and FT-IR spectroscopy) offer the advantages, by comparison with nonoptical techniques, of very rapid data acquisition and data reduction as well as having the potential for making multi-component measurements. The rapid signal-averaging rate (7) of the DOAS technique in particular, ensures that atmospheric scintillations are averaged out and there is therefore no need to enclose an air mass before analysis. Thus, labile species, or those in rapid photo-equilibrium, can be effectively studied with the DOAS system.

DOAS field studies are applicable to a wide range of atmospheric conditions. These include very clean background air measurements of, for example, HCHO and NO_2 (6) where optical pathlengths of > 10 km may be employed, as well as measurements in extremely polluted air for which pathlengths of a few hundred meters or less may be adequate. Thus, the criteria for pathlength selection are primarily the sensitivity required for a specific measurement and the extent of broad band atmospheric extinction.

High intensity, short arc xenon light sources provide useful photon fluxes in the spectral region from ~200 nm to > 700 nm. However, at the short wavelength end of this region, molecular scattering limits the maximum pathlength useable even in very clean air to < 1 km. At longer wavelengths (e.g., ~350 nm), scattering from particles in smoggy air also restricts the maximum light path. Fortunately, poor visiblity due to scattering from particles is usually associated with elevated levels of the nitrogenous pollutants and other species of interest and sufficient sensitivity is therefore still available for monitoring studies in photochemical air pollution episodes. Figure 1 illustrates the use of twin light sources at a monitoring site employed for HONO studies described below. Twin light sources not only provide some degree of spatial resolution but allow measurements to be conducted over a wider range of visibility conditions at the site.

Figure 2 illustrates the mobile field laboratory presently in use for DOAS studies at SAPRC. A monitoring site can be quickly established by one or two workers and the spectrometer system and associated instrumentation are as far as possible under automatic control, requiring only intermittent attention (once every 24-48 hours) by the operator. The collecting mirror shown in Figure 2 is under servo control of the DEC 11/23 minicomputer and dynamically maintains correct alignment for accurate viewing of the remote light source. In principle, reference spectra could be automatically acquired by rotating short (10 cm) absorption cells into the light beam at appropriate intervals, although at present this task must be performed by the operator.

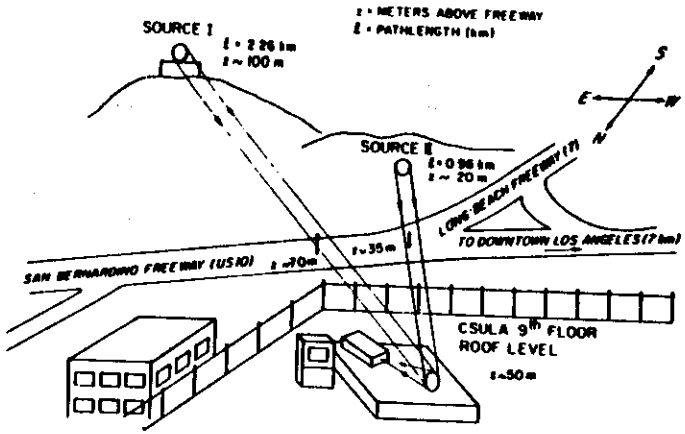

Fig. 1. DOAS field site near downtown Los Angeles with two light sources at different pathlengths

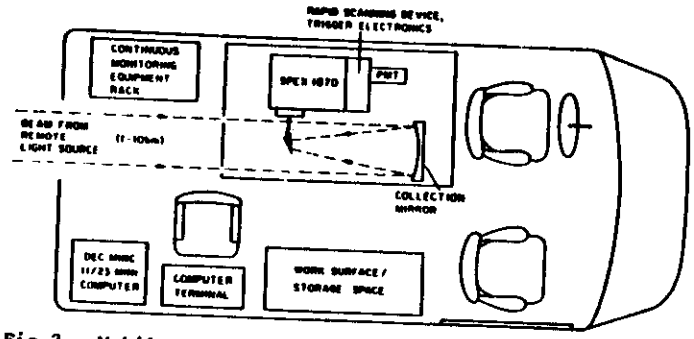

Fig. 2. Mobile van containing DOAS system and associated instrumentation

Subtraction of suitably weighted reference spectra of the strongest absorber may be performed automatically as described in the companion paper (7) and time-resolved optical density/concentration data output to mass storage and/or an X-Y recorder. Since not all the species of interest in a particular study have absorption structure in the same 40 nm wavelength region which the DOAS may monitor at any one time, the spectrometer is equipped with a stepper motor wavelength drive which may be directed by the computer to traverse the central wavelength pointer between regions of interest in a programmable sequence.

The following sections describe selected monitoring studies carried out with our DOAS instrumentation over the last two years in southern California and illustrate the chemical insight which may be obtained by such rapid, simultaneous, multi-component monitoring of clean and polluted air masses.

Measurements of the Nitrate Radical

Due to their free radical structure, NO and NO_2, usually referred to collectively as "NO_x," are active in many atmospheric trace gas cycles. However, in order to understand the chemical cycles of NO and NO_2, the

chemistry of a number of other nitrogen compounds, which play a role in the production, storage, conversion and sink mechanisms of NO_x have to be investigated as well. These species include the nitrate radical (NO_3), the nitrogen oxyacids (HNO_2 and HNO_3) and the anhydride of nitric acid (N_2O_5). The chemical cycles and reaction sequences involving the chemistry of these nitrogenous species (both during the day and at night) are complex. Since O_3 is usually present at night, NO is rapidly converted to NO_2 which in turn can react slowly with O_3 to form NO_3. The nitrate radical is itself in equilibrium with N_2O_5. While the homogeneous reaction of N_2O_5 with water is known to be very slow (11), the heterogeneous hydrolysis of N_2O_5 may be a major loss mechanism for NO_x at night and hence a potentially important nighttime source of HNO_3 (and acid rain).

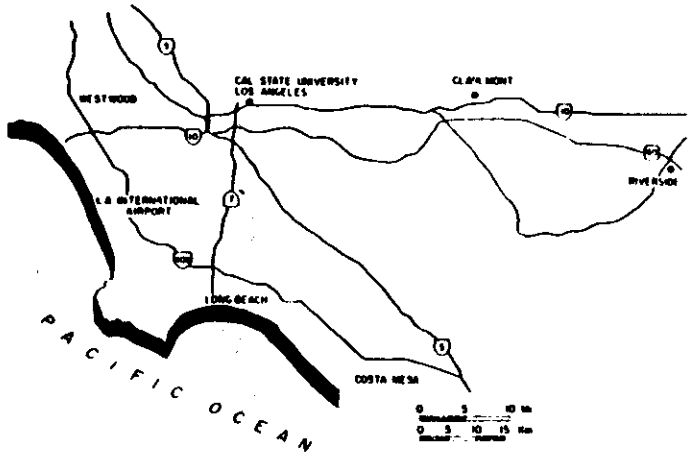

Fig. 3. A portion of the Los Angeles airshed including the Riverside, Claremont and downtown Los Angeles sites used in DOAS studies. Not shown is a desert site (Whitewater Hill) ~175 km due east of Los Angeles

Evidence for this mechanism is provided by our measurements of NO_3 time-concentration profiles at four sites in the Los Angeles airshed since August 1979. Studies were conducted at Riverside, Claremont and downtown Los Angeles (see Figure 3), sites usually experiencing air of comparatively high humidity, as well as at a desert site (Whitewater Hill north of Palm Springs) which generally experiences low relative humidities. Our first measurement program was carried out on a total of 15 days in August and September 1979 at Riverside and Claremont, using 970 and 750 m optical paths, respectively. Nitrate radical concentrations as high as 355 ppt were observed in nighttime measurements made at Riverside during an air pollution episode which persisted from September 11 to 19.

Figure 4 shows the development of the 623 and 662 nm NO_3 bands (monitored alternately in 10-minute intervals) on the evening of September 12, 1979. In both wavelength regions, water vapor absorption lines have been cancelled by subtracting early-morning reference spectra taken at times with no ozone (and therefore no NO_3) present. Both the shape and position of the observed bands agree very well with NO_3 reference spectra obtained by placing a 4 cm cell filled with a mixture of O_3 and NO_2 in the light beam, and with the spectrum reported by Graham and Johnston (12).

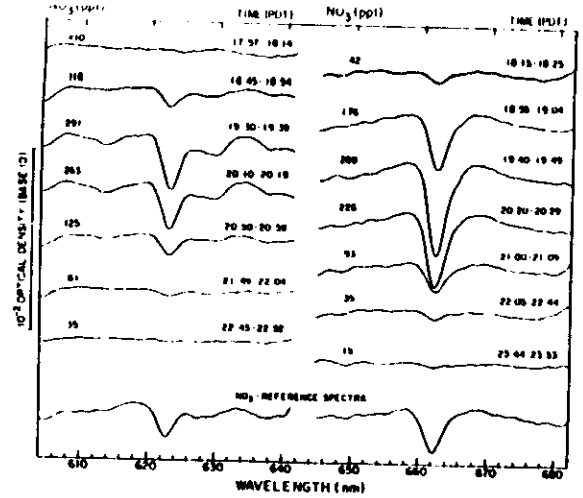

Fig.4. Observation of NO_3 absorption bands by differential optical absorption spectroscopy (8)

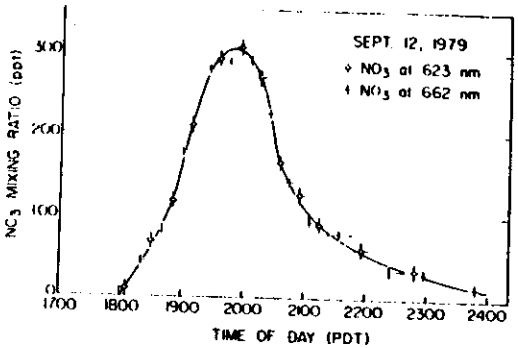

Fig.5. NO_3 time-concentration profile (Riverside, 970 m pathlength) (8)

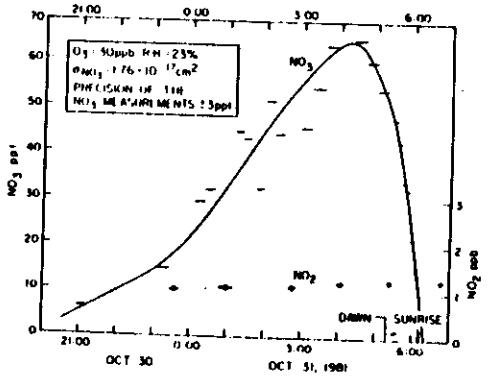

Fig.6. NO_3 night profile obtained with a 2.8 km lightpath at Whitewater Hill, desert site (14)

The concentration-time profile derived from the spectra given in Figure 4 is shown in Figure 5 along with the corresponding NO_2 and O_3 concentrations. Prior to sunset the NO_3 concentration was below the detection limit of ~5 ppt due to the short photolytic lifetime of the

nitrate radical (13). After sunset (~1800 PDT), the NO_3 concentration rose rapidly, peaking at ~2000, and then declined to levels below the detection limit after midnight. Similar behavior was observed on many other nights during this study at Riverside and Claremont. The detailed data from this investigation have been reported elsewhere (8).

Another extended set of measurements of ambient NO_3 concentrations was carried out at a desert site (Whitewater Hill) ~170 km east of downtown Los Angeles. These measurements yielded similar peak concentrations (up to 214 ppt) to those observed in the Riverside/Claremont study. However, the concentration-time profiles typically observed at Whitewater Hill (see Figure 6) were very different from those previously measured. In particular appreciable NO_3 concentrations were present throughout the night until dawn when the NO_3 concentration rapidly decreased to levels below our detection limit (14).

Taken together the results from these studies indicate that under conditions of high humidity (> 70%) the lifetime of the nitrate radical is very short (< 1 min) presumably due to the reaction of N_2O_5 with wet aerosol surfaces. On the other hand, for relative humidities below ~50% RH lifetimes as long as ~1 hour occur. Although lifetimes of NO_3 as short as ~1 hr could result from low concentrations of NO at the site, we are able to rule out this possibility using the multi-component monitoring capability of the DOAS technique. Specifically, if sufficient NO were present at the site to account for the observed NO_3 lifetime, then a large increase in the NO_2 concentration (due to the parallel reaction of NO with O_3) would have been observed with the DOAS system. Since this was not the case, we must conclude that a one-hour lifetime cannot be explained on the basis of our present understanding of NO_3 chemistry, suggesting that under dry conditions unknown sinks for NO_3 are operative (see Platt et al. (15). Similar conclusions have also been reached by Noxon et al. (16).

Measurements of Nitrous Acid

The importance of nitrous acid arises not only from its role as precursor for hydroxyl radicals, a key radical intermediate in photochemical cycles in both the clean and polluted troposphere, but also due to its facile reaction with secondary amines to form carcinogenic nitrosamines (17).

HONO is thought to be formed by two major pathways, the recombination of OH radicals with NO

$$OH + NO \xrightarrow{M} HONO \qquad (1)$$

and the direct reaction of nitrogen oxides with water

$$NO + NO_2 + H_2O \rightarrow 2\ HONO \qquad (2)$$

$$NO_2 + NO_2 + H_2O \rightarrow HONO + HNO_3 \qquad (3)$$

The latter reactions may proceed either homogeneously or heterogeneously. Reaction (1) proceeds only when significant concentrations of OH radicals are present (i.e., essentially only during daylight). However, the HONO concentrations during daytime are very low, due to its rapid photolysis, and correspond to a lifetime of ~10 min (8). At night in the absence of photolysis, higher concentrations of HONO can accumulate.

In a series of DOAS measurements beginning in the summer of 1979 at Riverside, Claremont and downtown Los Angeles, HONO was identified and

ly two hours.

This rapid photolysis of HONO at sunrise produces OH radicals, resulting in an ~2 hr "pulse" of radicals at a time when other sources of OH (e.g., O_3 and HCHO photolysis) are weak (9). Thus, HONO photolysis at sunrise can considerably accelerate the formation of photochemical air pollution and, in order to correctly model photochemical smog formation in urban airsheds, it is clearly necessary to have reliable data concerning HONO concentrations in the early morning hours.

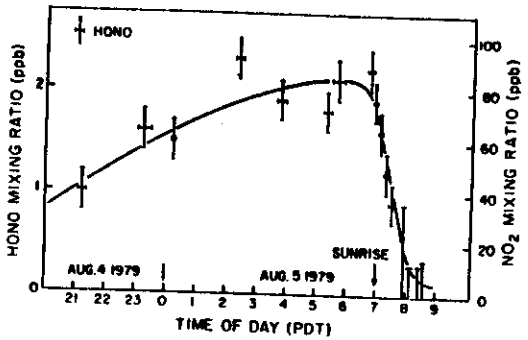

Fig.7. Concentration-time profiles of HONO and NO_2, 4-5 August 1979, Riverside, California (9)

Conclusion

During the past two years, the DOAS technique employed by researchers from the Institut für Chemie (Jülich) and the University of California Statewide Air Pollution Research Center (Riverside) has proven to be a versatile and powerful tool for practical studies of ambient concentrations of such critical species as HONO, NO_3 and HCHO under a wide variety of atmospheric conditions. The DOAS system has also been used to measure the concentrations of the criteria pollutants O_3, SO_2 and NO_2 in clean and polluted atmospheres over long pathlengths, in some cases in a more informative and cost effective manner than possible with point monitors.

In principle many other pollutants and atmospheric species which have structured absorption spectra in the UV, visible and near-IR regions can be identified and measured with the DOAS system. Efforts are underway in our respective laboratories to extend the applications of this instrument to other studies of the chemistry of the clean and polluted troposphere.

Acknowledgement

The authors gratefully acknowledge support of this work by the National Science Foundation (Grants No. PFR 78-01004-A01 and ATM-8001634).

1. E. C. Tuazon, R. A. Graham, A. M. Winer, R. R. Easton, J. N. Pitts, Jr. and P. L. Hanst, Atmos. Environ., 12, 865 (1978).

2. E. C. Tuazon, A. M. Winer, R. A. Graham and J. N. Pitts, Jr., Adv. Environ. Sci. Technol., 10, 259 (1980).

(Grant No. X-804340), Research Triangle Park, NC, [illegible].

4. E. C. Tuazon, A. M. Winer and J. N. Pitts, Jr., Environ. Sci. Technol., 15, 1232 (1981).

5. D. Perner and U. Platt, Geophys. Res. Lett., 6, 917 (1979).

6. U. Platt, D. Perner and H. W. Pätz, J. Geophys. Res., 84, 6329 (1979).

7. U. Platt and D. Perner, "Measurement of Atmospheric Trace Gases by Long Path Differential UV/Visible Absorption Spectroscopy," Presented at Workshop on Optical and Laser Remote Sensing, Monterey, CA, February 9-11, 1982 (preceeding paper).

8. U. Platt, D. Perner, A. M. Winer, G. W. Harris and J. N. Pitts, Jr., Geophys. Res. Lett., 7, 89 (1980).

9. U. Platt, D. Perner, G. W. Harris, A. M. Winer and J. N. Pitts, Jr., Nature, 285, 312 (1980).

10. G. W. Harris, W. P. L. Carter, A. M. Winer, J. N. Pitts, Jr., U. Platt and D. Perner, "Observation of Nitrous Acid in the Los Angeles Atmosphere and Implications for Predictions of Ozone-Precursor Relationships," Environ. Sci. Technol., in press (1982).

11. E. D. Morris, Jr. and H. Niki, J. Phys. Chem., 77, 1929 (1973).

12. R. A. Graham and H. S. Johnston, J. Phys. Chem., 82, 254 (1978).

13. F. Magnotta and H. S. Johnston, Geophys. Res. Lett., 7, 769 (1980).

14. U. Platt, G. W. Harris, A. M. Winer and J. N. Pitts, Jr., in preparation (1982).

15. U. Platt, D. Perner, J. Schöder, C. Kessler and A. Toennissen, J. Geophys. Res., 86, 11965 (1981).

16. J. F. Noxon, R. B. Norton and E. Marovich, Geophys. Res. Lett., 7, 125 (1980).

17. J. N. Pitts, Jr., D. Grosjean, K. Van Cauwenberghe, J. P. Schmid and D. R. Fitz, Environ. Sci. Technol., 12, 946 (1978).